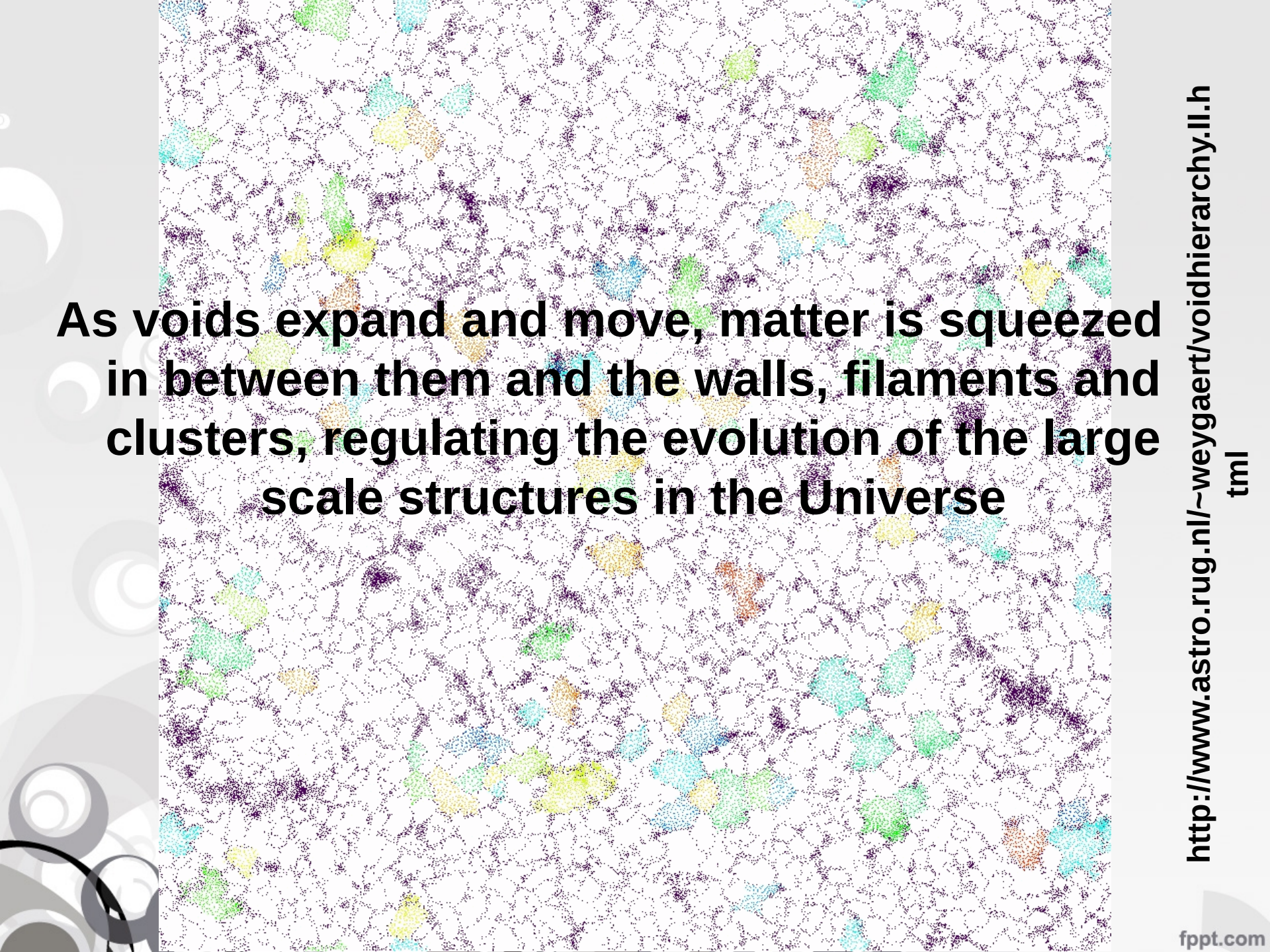


The motion of emptiness

Dynamics and evolution of cosmic voids

Laura Ceccarelli

IATE, Observatorio Astronómico de Córdoba

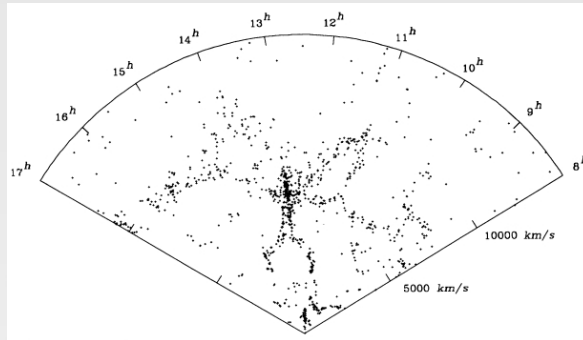


As voids expand and move, matter is squeezed in between them and the walls, filaments and clusters, regulating the evolution of the large scale structures in the Universe

Voids became evident on LSS

Voids appear in the galaxy distribution:
The CfA-II slice (de Lapparent, Geller & Hucha, 1986), reveals the large scale structure of the Universe.

A slice of the Universe



Evolution and dynamics:
Expansion

The two essential "void hierarchy modes"

- ◆ Void-in-void process: void growing through the merging of two or more smaller voids
- ◆ Void-in-cloud process: a void demolished through the gravitational collapse of embedding region.

It was extensively believed that voids were static components of the large scale universe

Bootes void (Kirshner et al. 1981)

A MILLION CUBIC MEGAPARSEC VOID IN BOÖTES?

ROBERT P. KIRSHNER^{1,2}
Department of Astronomy, University of Michigan

AUGUSTUS OEMLER, JR.^{1,2}
Department of Astronomy, Yale University

PAUL L. SCHECHTER¹
Harvard-Smithsonian Center for Astrophysics and Kitt Peak National Observatory³

AND
STEPHEN A. SHECTMAN¹
Mount Wilson and Las Campanas Observatories
Received 1981 March 30; accepted 1981 May 15

ABSTRACT

In the course of a redshift survey of galaxies brighter than $R \approx 16.3$, 133 redshifts were measured in three fields, each separated by roughly 35° from the other two. If the galaxies in these fields were distributed uniformly, the combination of a galaxian luminosity function and our magnitude limits predicts that the distribution of redshifts should peak near $15,000 \text{ km s}^{-1}$. In fact, only one galaxy of the 133 was observed with a redshift in the 6000 km s^{-1} interval centered on $15,000 \text{ km s}^{-1}$. One plausible interpretation is that a large volume in this region of order 10^6 Mpc^3 is nearly devoid of galaxies.

Two essential processes on void evolution determined by the surrounding global density: Expansion and collapse

Mon. Not. R. Astron. Soc. **350**, 517-538 (2004)

doi:10.1111/j.1365-2966.2004.07661.x

A hierarchy of voids: much ado about nothing

Ravi K. Sheth^{1*} and Rien van de Weygaert^{2*}

¹Department of Physics and Astronomy, University of Pittsburgh, 3941 O'Hara St., Pittsburgh, PA 15260, USA

²Kapteyn Institute, University of Groningen, PO Box 800, 9700 AV Groningen, the Netherlands

Accepted 2004 January 21. Received 2004 January 20; in original form 2002 August 1

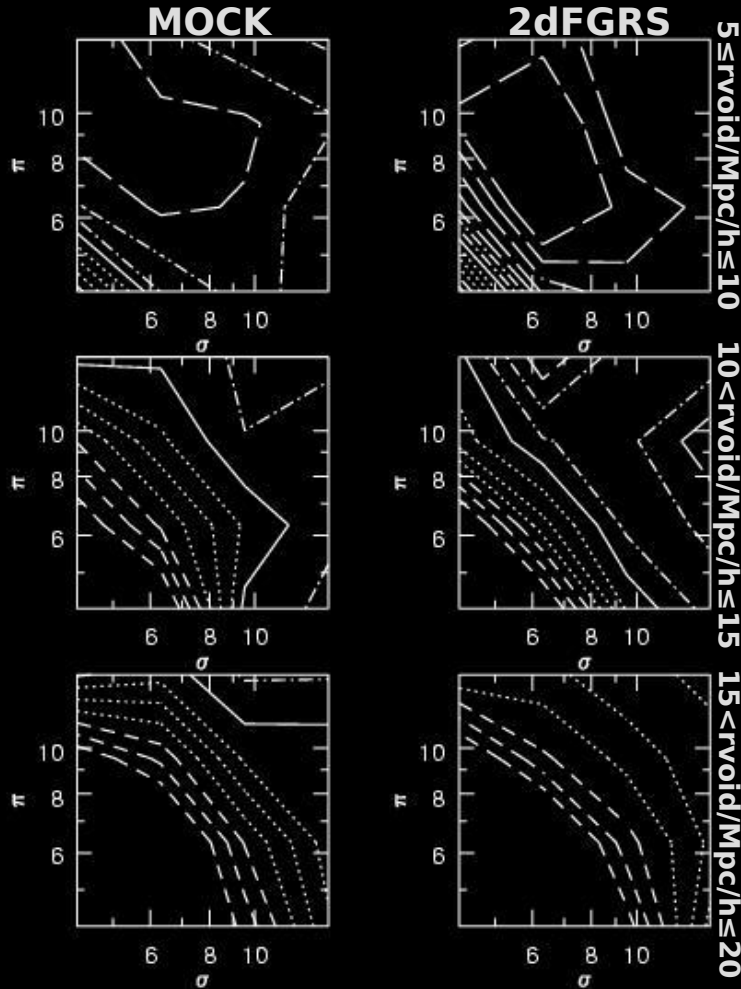
ABSTRACT

We present a model for the distribution of void sizes and its evolution in the context of hierarchical scenarios of gravitational structure formation. We find that at any cosmic epoch the voids have a size distribution that is well-peaked about a characteristic void size that evolves self-similarly in time. This is in distinct contrast to the distribution of virialized halo masses, which does not have a small-scale cut-off.

In our model, the fate of voids is ruled by two processes. The first process affects those voids which are embedded in larger underdense regions: the evolution is effectively one in which a larger void is made up by the mergers of smaller voids, and is analogous to how massive clusters form from the mergers of less massive progenitors. The second process is unique to voids, and occurs to voids that happen to be embedded within a larger-scale overdensity: these voids get squeezed out of existence as the overdensity collapses around them. It is this second process which produces the cut-off at small scales.

In the excursion set formulation of cluster abundance and evolution, the solution of the *cloud-in-cloud* problem, i.e. counting as clusters only those objects which are not embedded in larger clusters, requires the study of random walks crossing *one barrier*. We show that a similar formulation of void evolution requires the study of a *two-barrier* problem: one barrier is required to account for voids surrounded by the other barrier, the *low* barrier, and the other barrier is required to account for voids surrounded by the other barrier, the *high* barrier. The two barriers are the formation of voids, and the other the formation of collapsed objects.

Void dynamics from redshift space distortions



z-space void-glx correlation function $\xi(\sigma, \pi)$
 estimated from mock (left) and 2dFGRS (right)

Anisotropies in π direction
 ↓
 line of sight velocities

Compressed iso-density curves ► infall velocities

Elongated iso-density curves
 ► outflow velocities

We model the distortions on the void-galaxy cross-correlation function in z-space to obtain the velocity field around voids using the non-linear approximation:

$$V_{\text{inf}} = -\frac{1}{3} \frac{\Omega^{0.6} H_0 r \delta(r)}{[1 + \delta(r)]^{0.25}}$$

Anisotropies consistent with divergent velocity fields

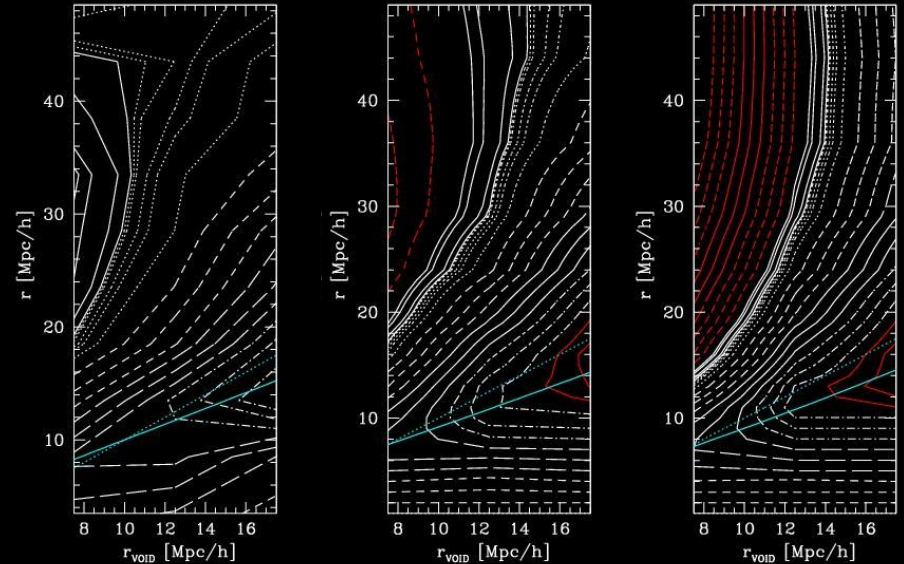
EXPANSION OF VOIDS

Predicted velocity field around voids applying the non-linear model to redshift space distortions

Mean velocity as a function of distance to the void centre.

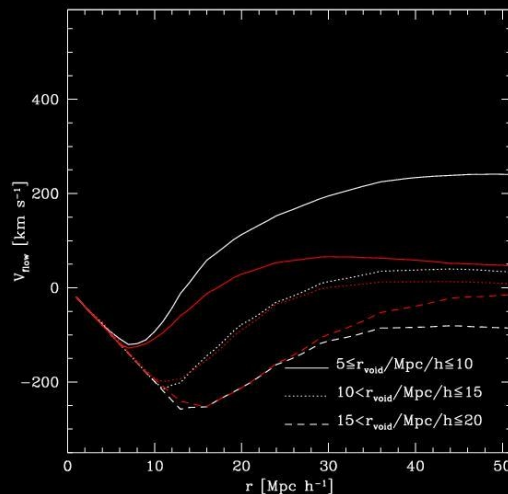
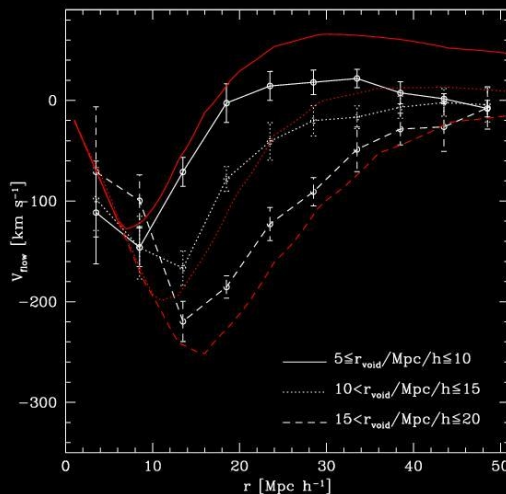
Left panel: predicted (red) and derived (white) velocities for mock.

Right panel: Predictions for the 2dFGRS (white) and mock (red).



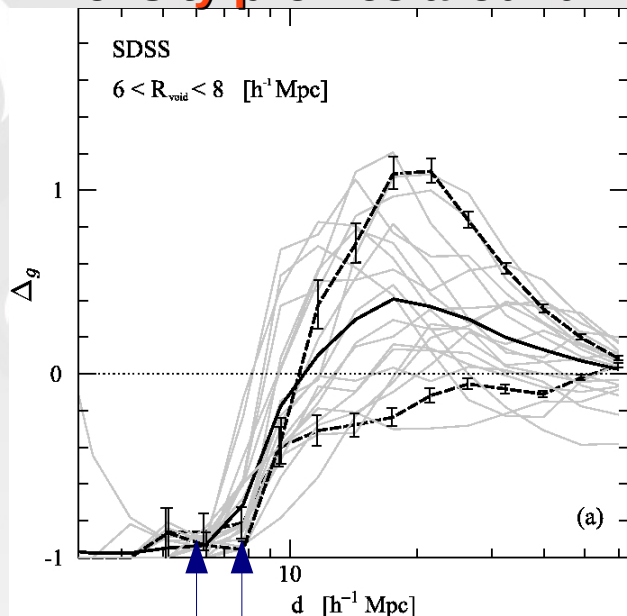
Contour lines of mean velocities as a function of void radius (x-axis) and distance to the void center (y-axis) modeled for 2DFGRS and mock and derived for mock (right, middle and left).

First estimations of expansion velocity for observational voids



Relative abundance of voids embedded in overdense environments for different void sizes in the galaxy distribution.

Density profiles around voids



It is possible to classify voids according to their large-scale density around them allowing for a subdivision of the sample into two types of voids

Integrated density contrast inside voids < -0.9

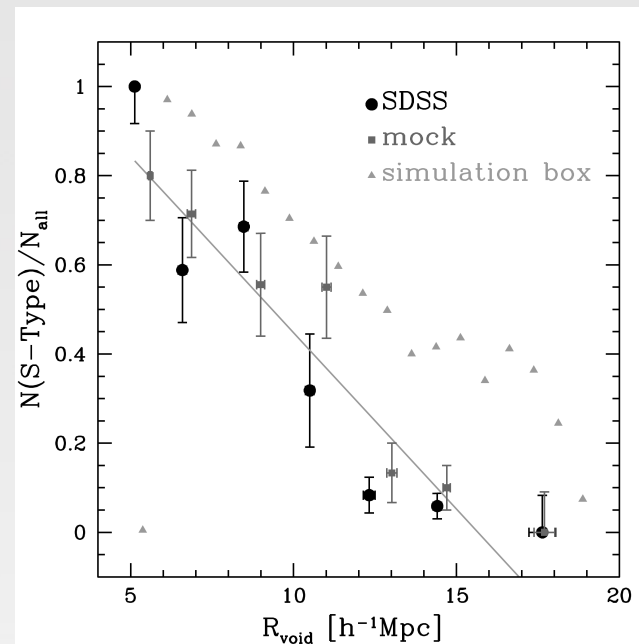
Void Classification

based on large scale environment

Large-scale “Shell” Profile \Rightarrow S-type voids

Large-scale “Rising” Profile \Rightarrow R-type voids

Clues on void evolution I. Ceccarelli, Paz, Lares, Padilla & Lambas. 2013, MNRAS, 434, 1435.



Small voids are more frequently surrounded by overdense shells.

Larger voids are more likely classified as R-Type.

The fraction of voids surrounded by overdense shells continuously decreases as the void size increases.

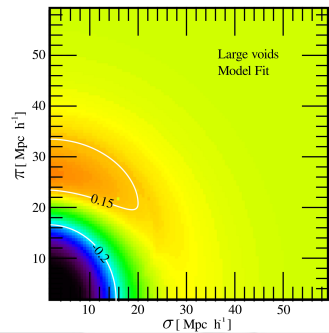
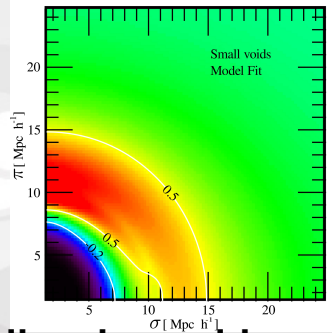
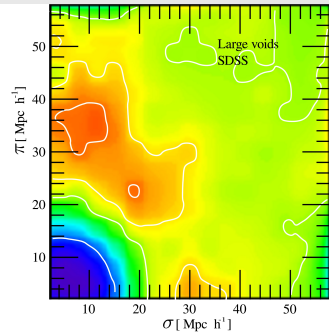
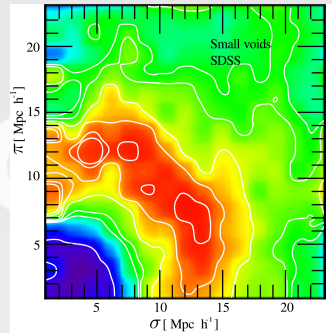
Dynamics around voids vs large scale environment

Redshift space distortions in observational data

Model results in observational data

Overdense environment

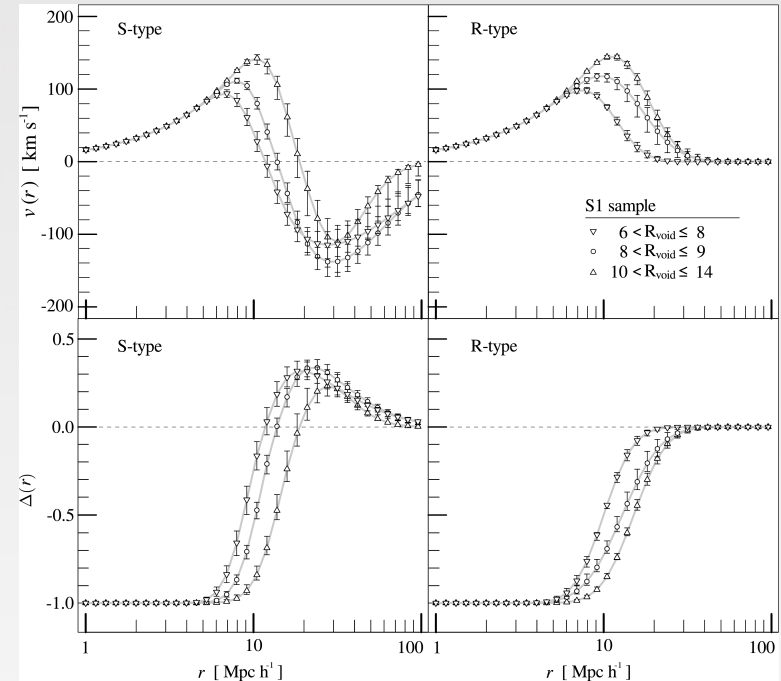
Underdense environment



Collapsing voids

Expanding voids

Velocity field



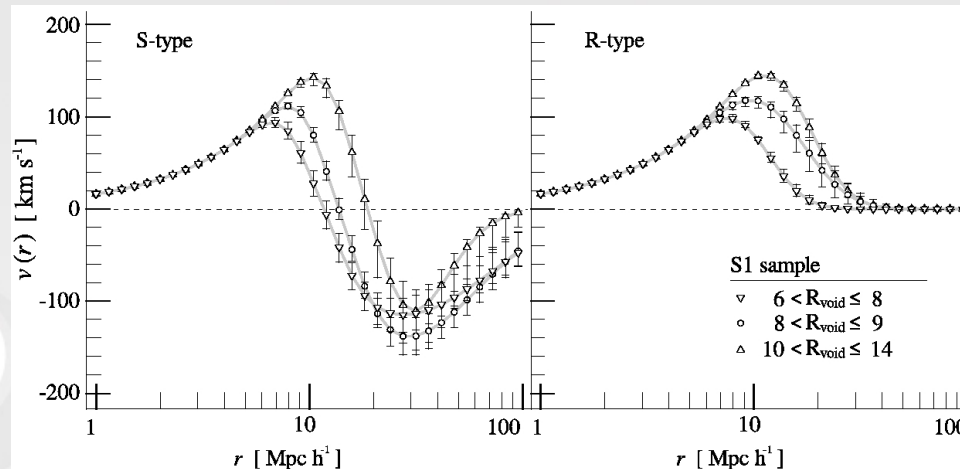
Density profile

Anisotropies in $\pi \rightarrow$ line of sight velocities
 Compressed iso-density curves \blacktriangleright infall velocities
 Elongated iso-density curves \blacktriangleright outflow velocities

As expected from theoretical predictions!

Dynamics around voids vs large scale environment

Radial peculiar velocity fields in observational data SDSS results



Voids in dense large-scale regions: inner regions are in expansion, the large-scale void walls are collapsing

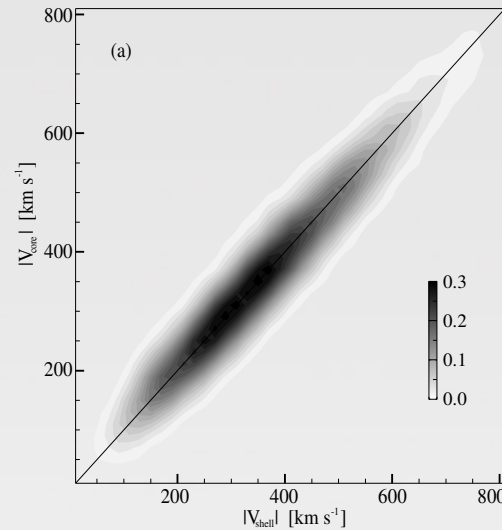
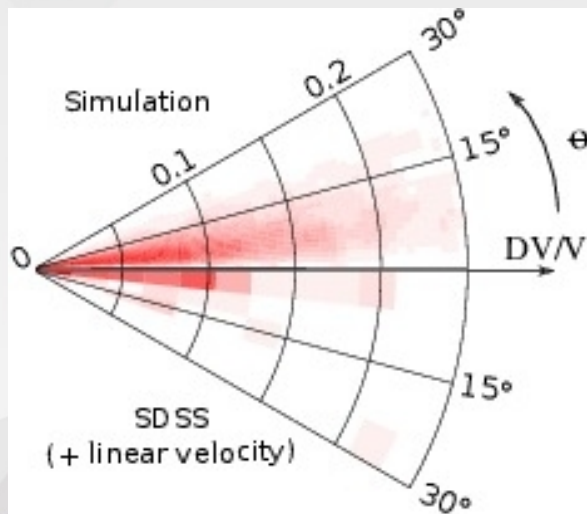
Voids in under-dense large-scale regions are in expansion

The first observational evidence of the two processes involved in void evolution

Void motions

Bulk velocities of void shells and cores

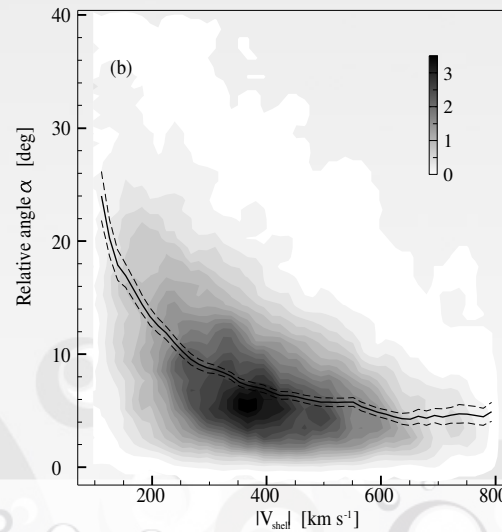
The dark matter in the void inner region and the haloes in the surrounding shell exhibit remarkably similar velocities (in magnitude and direction).



Bulk velocities of void shells and cores in the simulation.

V_{shell} : dark matter haloes mean velocity within $0.8 < r/R_{\text{void}} < 1.2$.

V_{core} : mean of dark matter particles within $0.8 R_{\text{void}}$.



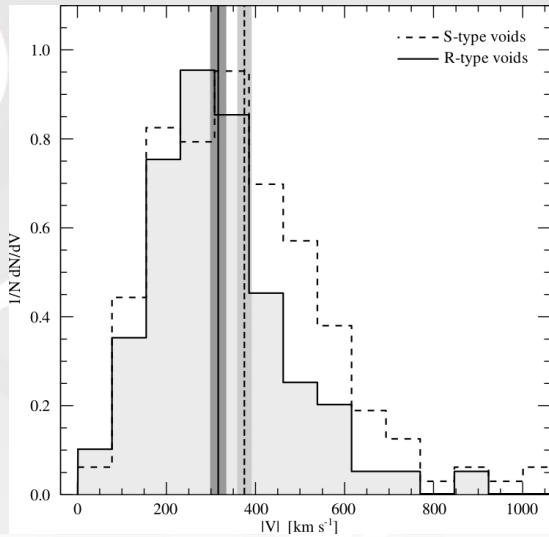
Upper: Distribution function of void counts in V_{shell} , V_{core} bins. Solid line shows the one-to-one relation.

Lower: Distribution function of void counts in bins of V_{shell} and the relative angle α between shell and core velocities. Solid and dashed lines correspond to the median and its standard error.

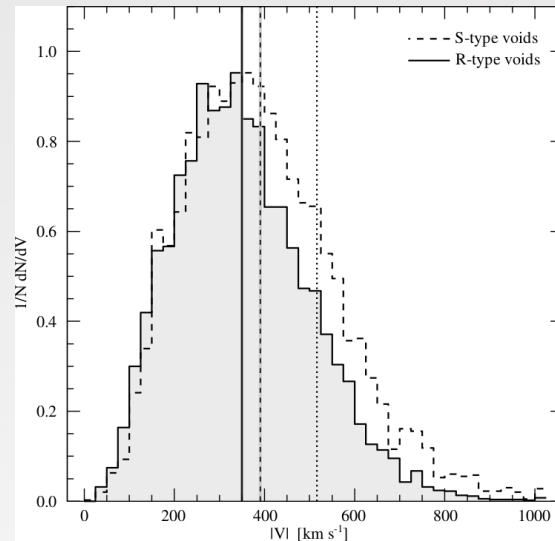
Void inner material and the surrounding haloes have a global common motion.

Void Bulk Motions

Void velocity normalized distributions for voids in SDSS.



Void velocity normalized distributions for the numerical simulation. Solid (dashed) line represents voids in under (over) dense regions. Vertical lines and bands show the corresponding mean velocities and standard errors (350 and 390 km/s). Dotted line indicates the mean velocity of haloes having $M > 10^{12} M_{\odot}/h$ (515 km/s).



Velocities in observational data

We have adopted the peculiar velocity field derived from linear theory by Wang et al. 2012. They use groups of galaxies as tracers of dark matter halos and its cross correlation function with mass, in order to estimate the matter density field over the survey domain. The linear relation between mass overdensity and peculiar velocity is used to reconstruct the 3D velocity field.

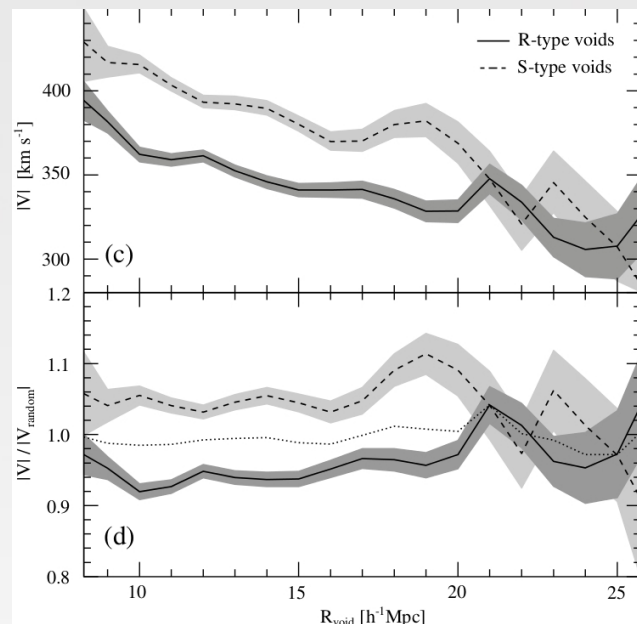
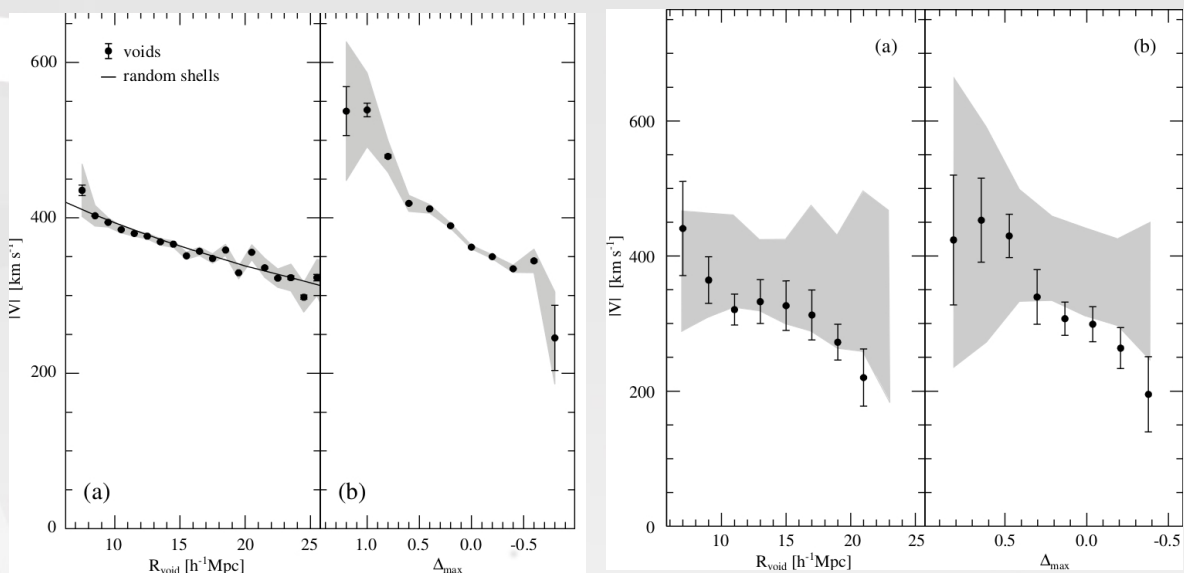
$$v(r) \approx -Hr\Delta(r) \frac{\Omega_m^{0.6}}{3}$$

It is remarkable that mean void and halo velocities are of the same order despite their very different nature, haloes being the most compact, extremely dense objects, and voids the largest empty regions in the Universe

Void Motion

Mean velocity for voids as a function of void radii (left) and Δ_{\max} (right), for simulation and SDSS.

Upper: Mean velocity as a function of the void radius for voids *en* over (dashed line) and under (solid line) dense regions in the simulation. Lower: Ratio between the velocities of void and random spheres.



Void velocities tend to be smaller as void size increases.

Smaller voids ($r_{\text{void}} < 8$ Mpc/h) exhibit velocities as large as 400 km/s and this velocity decreases to 300 km/s for the largest voids ($r_{\text{void}} > 17$ Mpc/h).

There is a clear trend of void velocities to be larger as surrounding density increases.

Besides the dependence of void size with the density of the region surrounding the void, the magnitude of mean void velocity is related with both, void size and environment.

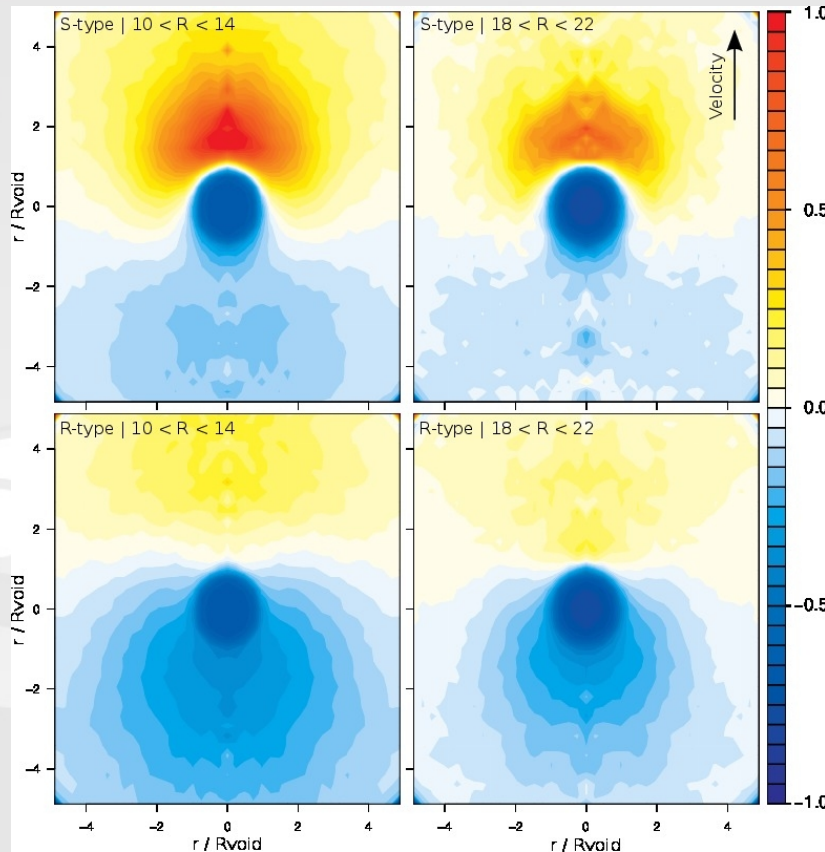
Void Bulk Motions

Voids in overdense environments

S-type voids

Voids in underdense environments

R-type voids

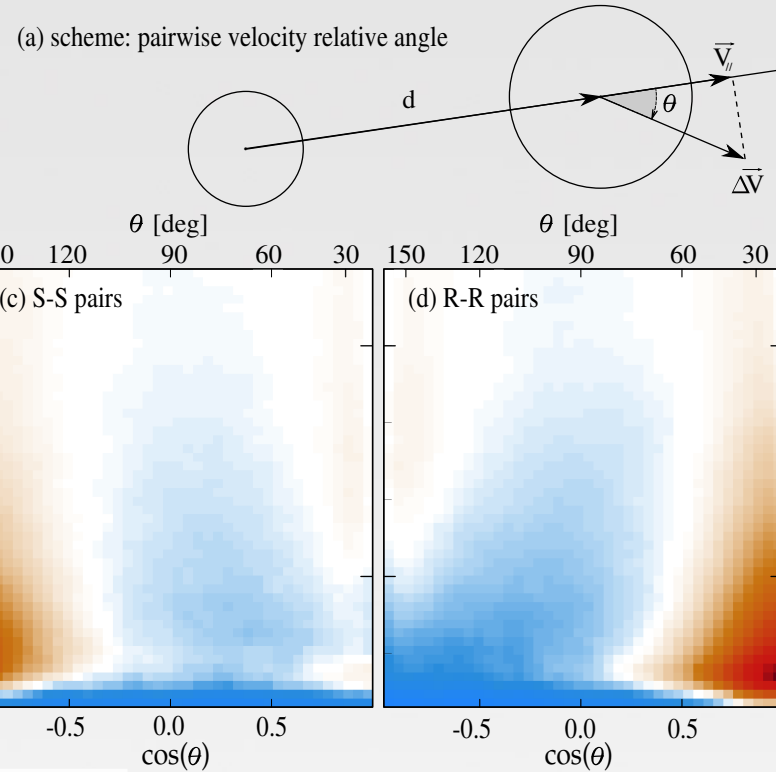
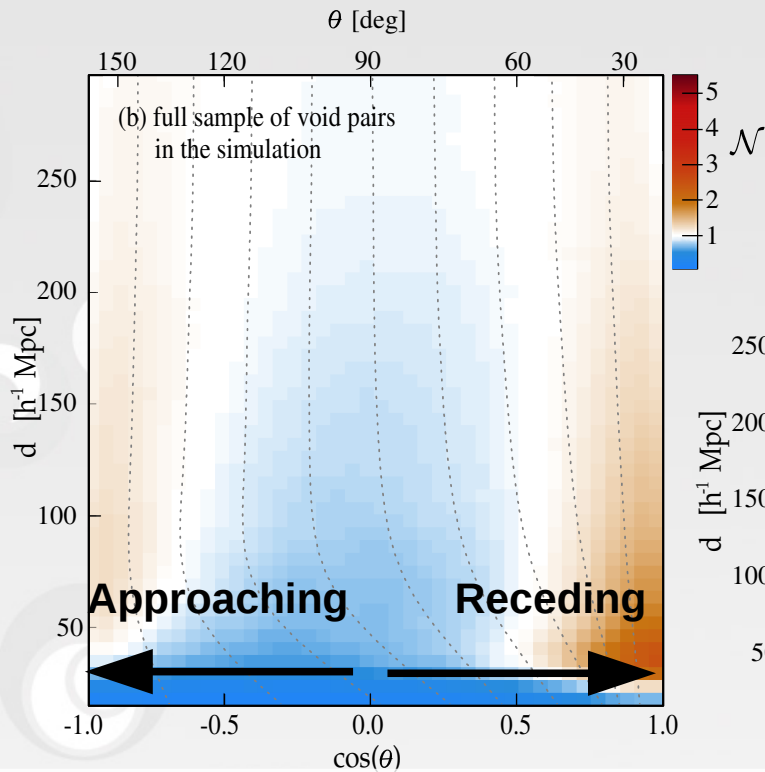


Density maps of stacked voids, the y-axis direction correspond to the void velocity vector. Overdensity increases from blue to red and white color correspond to the mean density.

There is a remarkable overdensity in the direction of velocity whereas in the opposite it is observed an underdensity

Voids seem to be abandoning low dense regions and moving to overdensities

The coherent motions of cosmic voids



the angle between the void relative velocity and the void relative separation vectors exhibits two peaks,

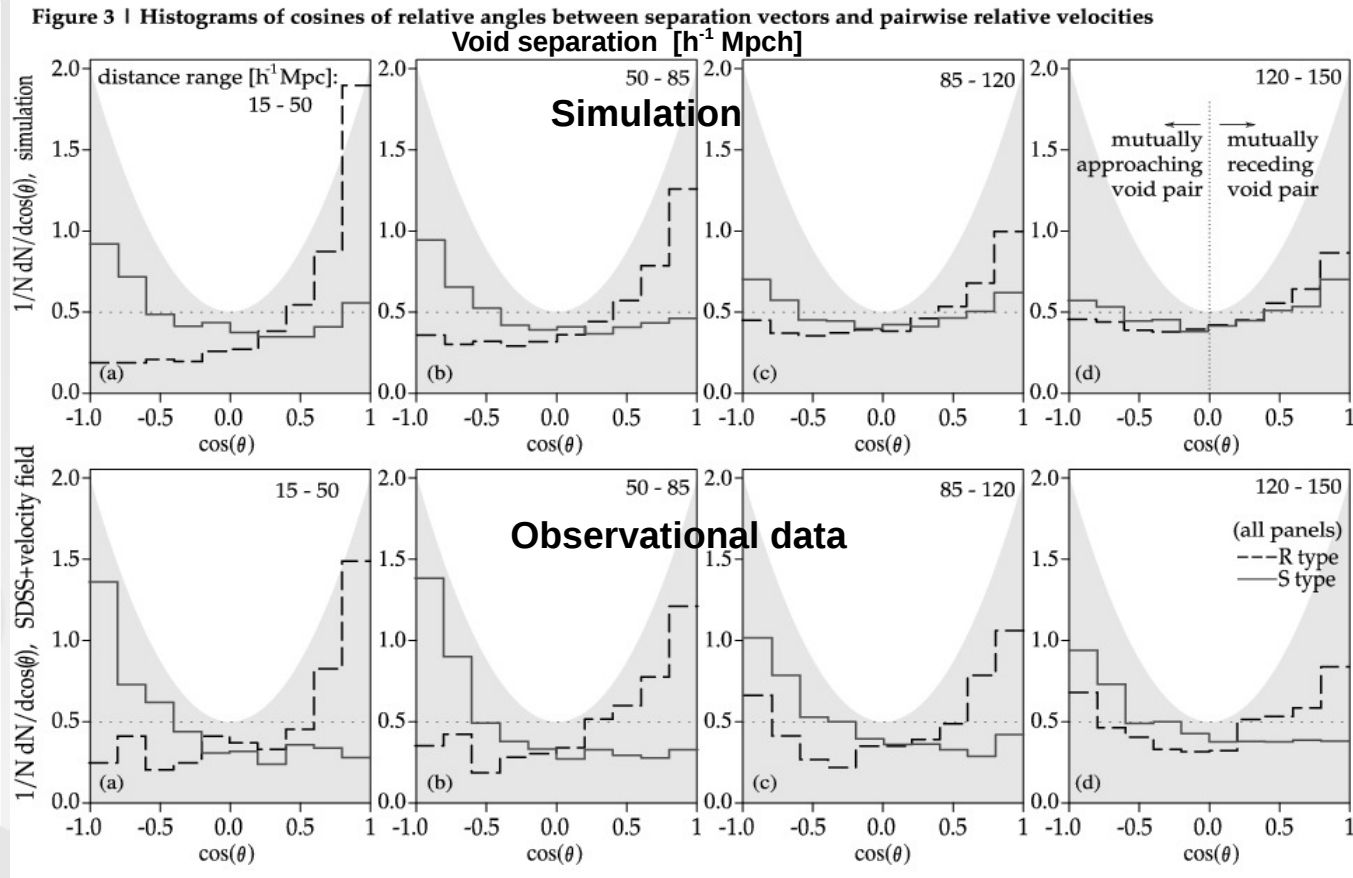
showing the presence of two populations with voids mutually receding and approaching

S-type void pairs are systematically approaching each other while R-type voids are mutually receding

The coherent motions of cosmic voids

Bimodality of relative motions in observational data.

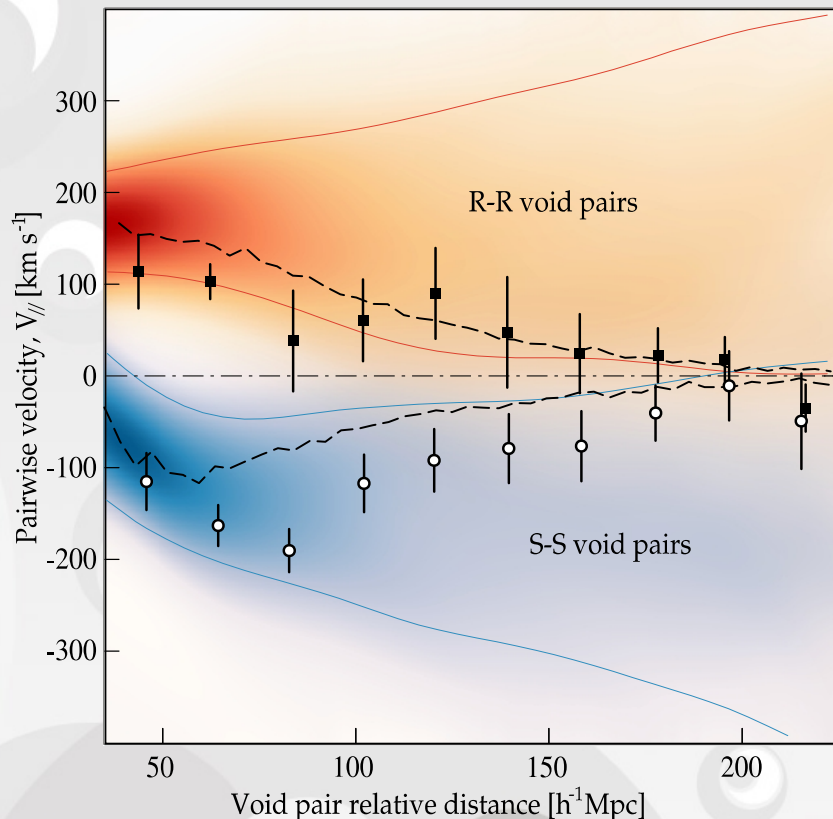
Histograms of $\cos(\theta)$ for different void pair separations ranges in underdense (dashed) and overdense (solid) environments (R and S-types, respectively). We show for reference a quadrupolar distribution with arbitrary normalization. Histograms are normalized to show the excess of void pairs with respect to the expectation from a random distribution.



The bimodality in observational data is consistent with the prediction of the Λ CDM model.

Two populations with voids mutually receding and approaching in observational data

The coherent motions of cosmic voids



Mean pairwise velocity values of the observational voids as a function of void relative separation.

The colour density map correspond to the results of R-R (red) and S-S (blue) void pairs in subboxes taken at simulation constrained to account cosmic variance in SDSS.

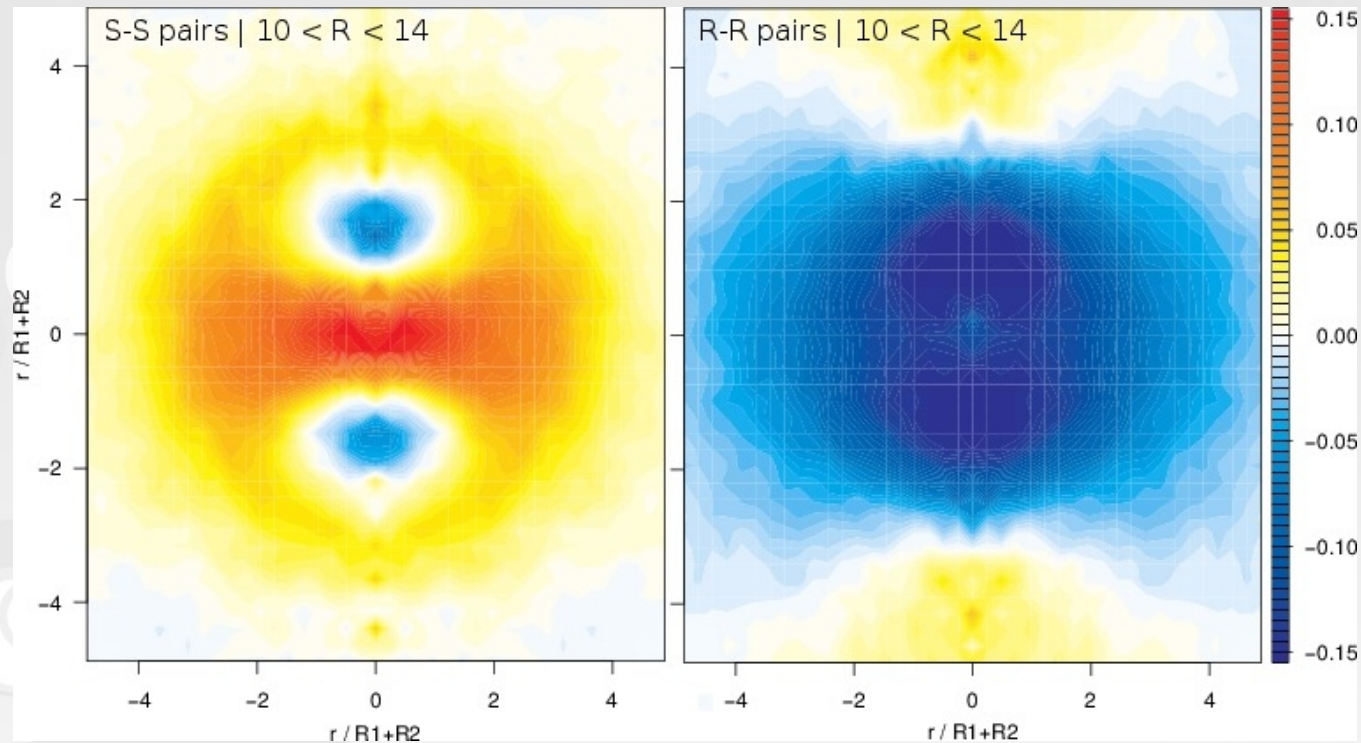
The thin blue and red lines correspond to the 0.16 and 0.84 quantiles of the distribution of $V_{||}$, for S-S and R-R void pairs, respectively.

The thick dashed lines correspond to the full simulation box results for R-R and S-S pairs. Points represent SDSS results.

The observational results are entirely consistent with the prediction of the Λ CDM model.

Voids behave either receding or approaching each other according to their R/S-type classification with velocities of the order of 100–150 km/s up to 200 Mpc/h separation.

The coherent motions of cosmic voids



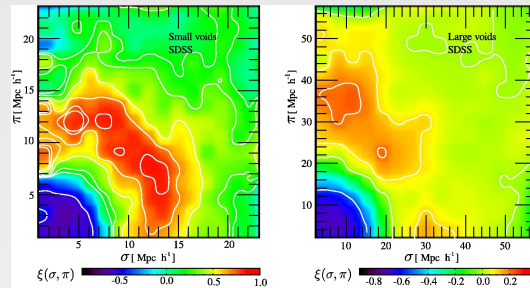
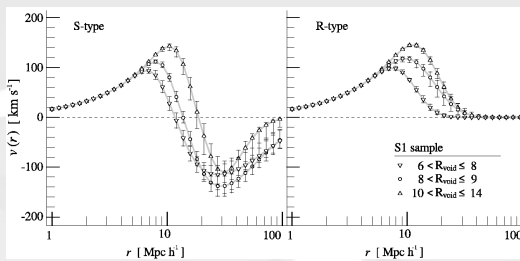
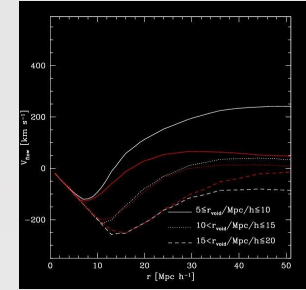
Staked mass density for S-S and R-R void pairs. The y-axis is oriented to the velocity difference direction.

As this direction is aligned with the relative separation direction, the coherent pattern emerges

Summary: Our contributions to void dynamics

→ We obtained the first estimations of the velocity field around observational voids (Ceccarelli et al. 2006).

→ We obtained the first observational evidence of a twofold population of voids according to their dynamical properties as predicted by theoretical considerations (Ceccarelli et al. 2013, Paz et al. 2013, Ruiz et al. 2015).



→ We reported the bimodality on void pairwise velocities (Lambas et al. 2016).

→ We reported by first time on the significant motions of cosmic voids as a whole and studied the coherence pattern associated to the void velocity field up to large cosmological scales, both in simulations and observations (Ceccarelli et al. submitted, Lambas et al. 2016).

